Proceedings of International Conference on Technology and Social Science 2018 (ICTSS 2018)
KEYNOTE

Properties of N-doped Sb_2Te_3 Film and Its Application to Artificial Intelligence Synaptic Device

You Yin[a], Ryoya Satoh and Keita Sawao

Division of Electronics and Informatics, Faculty of Science and Technology, Gunma University,

1-5-1 Tenjin-cho, Kiryu 376-8515, Japan

[a]<yinyou@gunma-u.ac.jp>

Keywords: chalcogenide, phase change, memory, artificial intelligence, synaptic device

Abstract. In this work, we investigated sputtered undoped and N-doped Sb_2Te_3 films by x-ray diffraction and resistance measurements. The application to artificial intelligence synaptic device is presented as well. Mean crystal size decreased from 6.8 to 2.9 nm and thus crystal growth was significantly suppressed by fine nitrides due to N-doping. The resistivity of as-deposited N doped Sb_2Te_3 could be around 2-3 orders of magnitude higher than that of undoped Sb_2Te_3 film. The N doped Sb_2Te_3 artificial intelligence synaptic device exhibited nonvolatility from the measured electrical characteristics because the states induced by current sweeping were very stable. The increase and decrease of conductance corresponding to the long-term potentiation and depression of synaptic weight, were demonstrated by current sweepings and voltage pulses, respectively.

1. Introduction

More and more complex information is required to be processed in the internet of things (IoT) era. Current computers are based on von Neumann architecture, which consumes much power especially when it is used for image and audio processing. This processing can be conducted efficiently with ultralow power and ultrahigh speed by brain-like computers for artificial intelligence (AI) based on parallel processing [1]. These promising computers are composed of artificial neurons and synapses. Synaptic devices are very important for these future's computers because the information is processed and stored in these devices and their number is 10^2~10^4 times that of neurons in our brain [2]. In recent years, some synaptic devices were demonstrated using materials such as Mn:HfO_2 [2], AgS [3], NiOx [4] and so on. However, they did not exhibit sufficiently good endurance, good retention and ultrafast speed for the application to artificial intelligence synaptic device. Chalcogenide materials, which are used for phase-change memory, showed almost perfect performance such as excellent endurance, low power, ultrafast speed, and nonvolatility [5-9]. In this work, we tried to investigate N-doped Sb_2Te_3 chalcogenide films and apply them to AI synaptic device for realizing synaptic plasticity, which is the most important characteristics for synaptic devices and makes it possible to adjust synaptic weight with applied pulses.

2. Experimental Methods

A series of 200 nm thick N-doped Sb_2Te_3 and Sb_2Te_3 film samples with a thin SiO_2 capping layer on a glass substrate was prepared by introducing both Ar and N_2 into the chamber using a radio frequency sputtering equipment (MNS-3000-RF, ULVAC, Inc.) at a background pressure below 5×10^{-5} Pa and a sputtering pressure of 0.2 Pa. Resistivity as a function of annealing temperature of films was measured by using square-shaped film samples ($12\times12\,\mathrm{mm}^2$) defined by Ti electrodes. The sample was annealed on a hot plate at each increasing temperature for 3 min. Crystal structures of films were characterized by X-ray diffractometer (RINT 2000, Rigaku co.) after annealed on a hot plate for 3 min. Current-voltage (*I*-*V*) characteristics of the device samples were measured by semiconductor parameter analyzer (4200-SCS, Keithley).

3. Characteristics of N-doped Sb_2Te_3 Film

Fig. 1 shows X-ray diffraction patterns of sputtered undoped and N doped Sb_2Te_3 (N_2 gas flow rate: 1 sccm) films at different annealing temperatures. As shown in Fig. 1(a), the face-centered cubic (fcc) crystal was found in as-deposited Sb_2Te_3 film. Sb_2Te_3 should have a low crystallization temperature of about 100^{o}C. The crystallites formed during sputtering because the sample might be heated up to above the crystallization temperature of Sb_2Te_3 without cooling sample holder. Only the fcc crystal structure was detected in Sb_2Te_3 films annealed at below 200 ^{o}C. A hexagonal (hex) crystal structure was appeared from the annealing temperature of 250 ^{o}C. The transformation of crystal structure from fcc to hex can be clearly known from the peak at an angle of 38.4^o. Compared with Sb_2Te_3 film, N-doped film showed that it was amorphous even when it was annealed at a temperature of 200 ^{o}C, as shown in Fig. 1(b). Crystallization to a fcc structure was occurred when it was annealed at temperatures of 250 and 300 ^{o}C. A transformation from fcc to hex was finally observed at an annealing temperature of 350 ^{o}C. Crystal size as a function of N_2 flow rate during sputtering is shown in Fig. 2. Crystal size decreased with doping N into Sb_2Te_3. Mean crystal size decreased from 6.8 to 2.9 nm and thus crystal growth was significantly suppressed by fine nitrides due to N-doping.

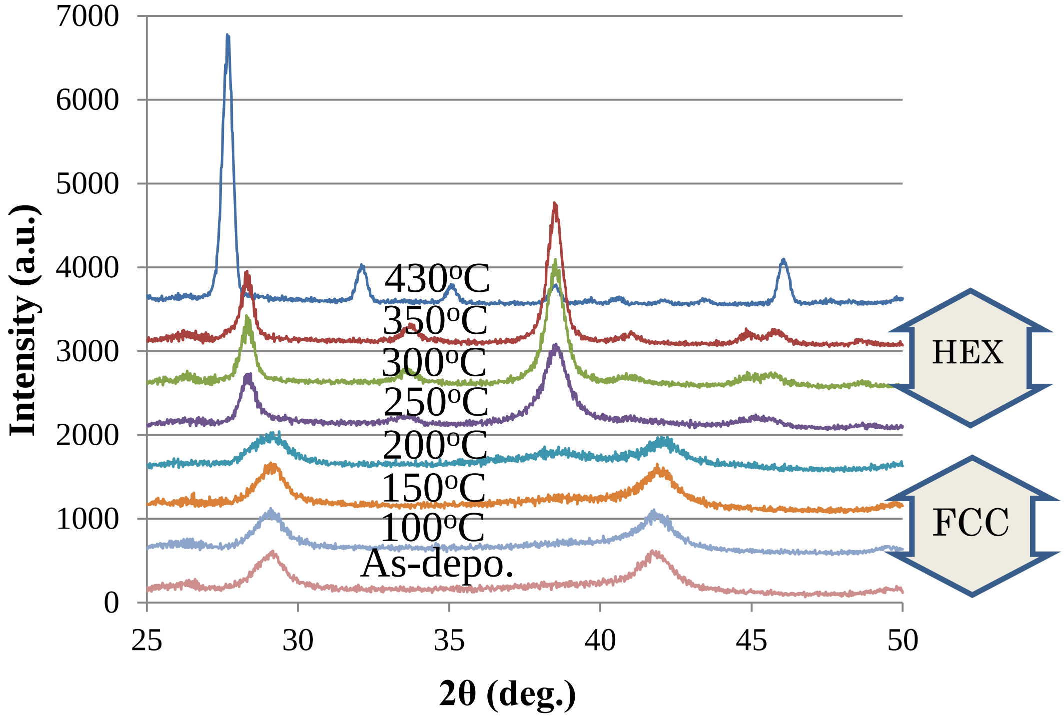

(a)

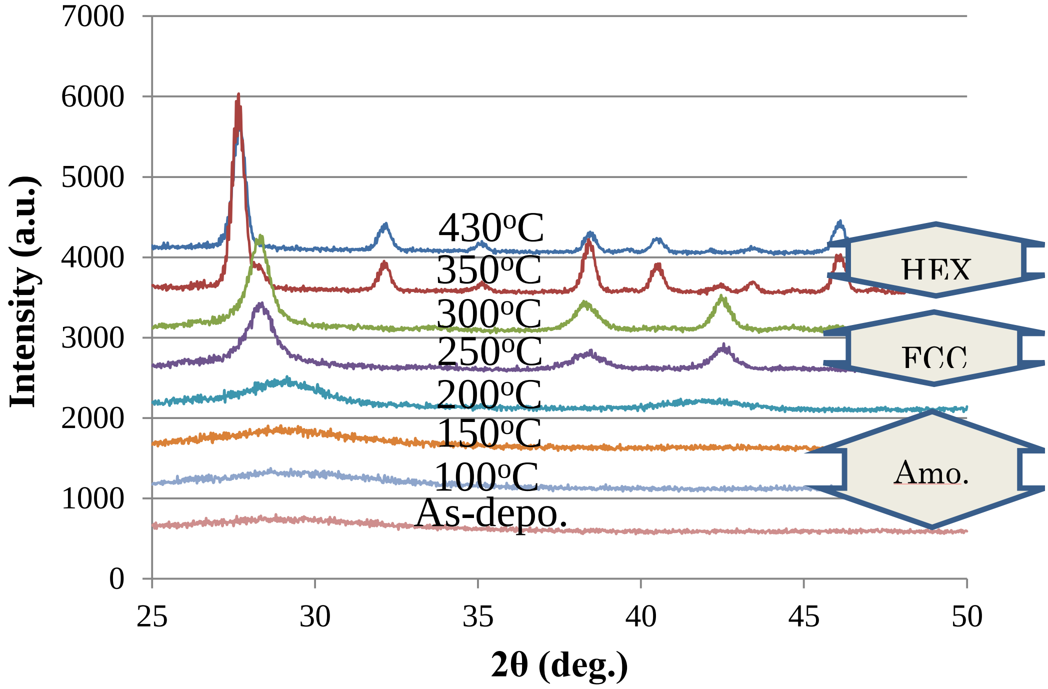

(b)

Fig. 1 X-ray diffraction of (a) Sb_2Te_3 film and (b) N-doped Sb_2Te_3 film

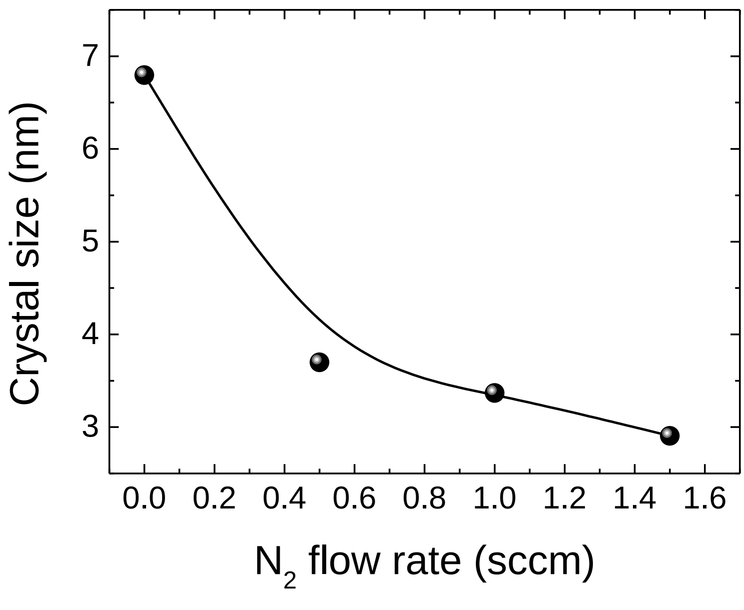

Fig. 2 Crystal size as a function of annealing temperature

Fig. 3 shows the resistivity of undoped (STN0.0) and N doped Sb_2Te_3 (STN0.5-STN3.0) films at different annealing temperatures. The resistivity of as-deposited undoped film was about 3×10^{-3} Ωm. The resistivity dropped to about 3×10^{-4} Ωm after the film was annealed at 250 ºC. The resistivity of as deposited N doped Sb_2Te_3 films was about 0.7–20 Ωm, 2 or 3 orders of magnitude higher than that of undoped Sb_2Te_3 films. This strongly depended on N_2 flow rate. All of these films showed a gradual resistivity drop due to crystallization to fcc and then to hex as described above.

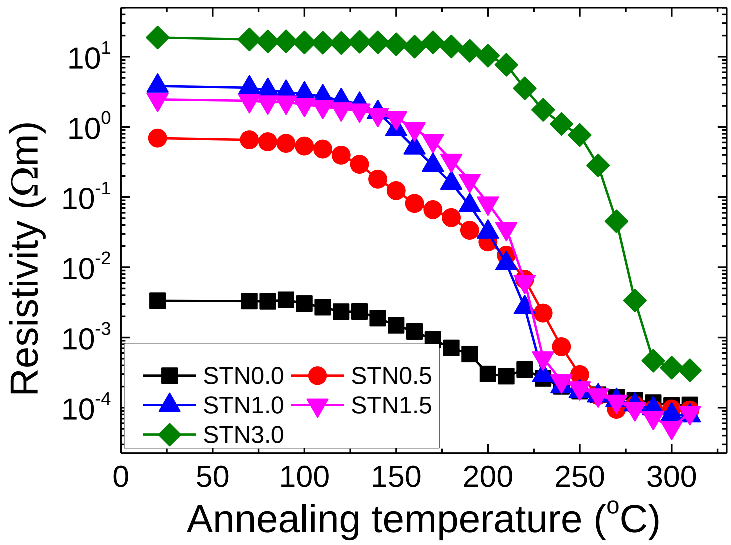

Fig. 3 Resistivity as a function of annealing temperature

4. Synaptic device for AI application

Fig. 4 shows the programming current-voltage (*I*-*V*) characteristics of the synaptic device by the current sweepings from 0 to the programming currents I_p forward and backward. The active layers of the device consisted of 150-nm-thick N-doped Sb_2Te_3 layer and a top 50-nm-thick TiN layer, as shown in the inset of Fig. 4. A protective insulator layer is 250-nm-thick ZnS-SiO_2. These layers were all deposited using a radio frequency sputtering equipment (MNS-3000-RF, ULVAC, Inc.) at a sputtering pressure of 0.2 Pa. The programming currents were from 0 to 2 mA with an increase of 0.1, 0.2 or 0.3 mA.

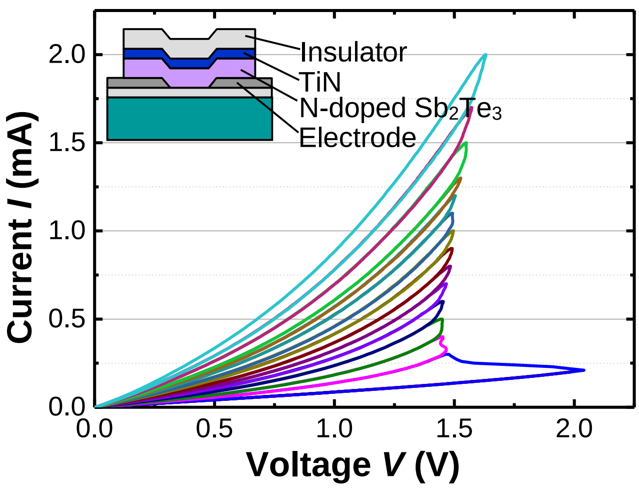

Fig. 4 *I*-*V* characteristics

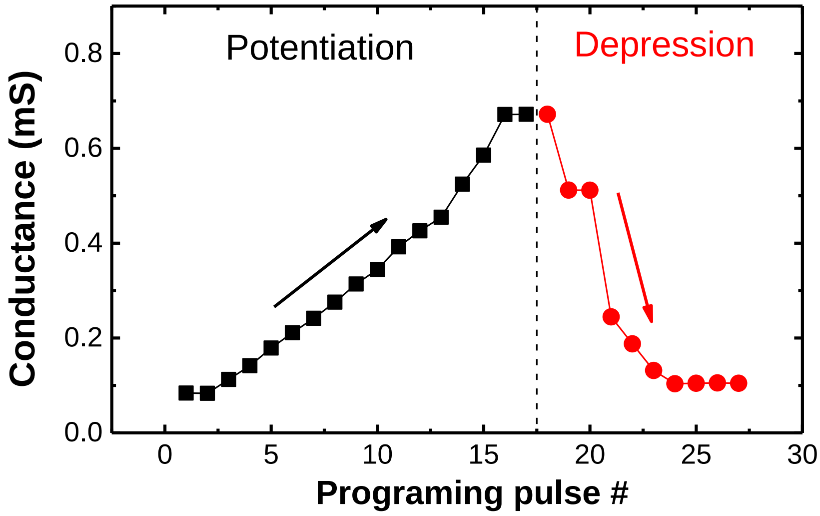

Fig. 5 The long-term potentiation and depression of synaptic weight

The synaptic device exhibited nonvolatility from the measured *I-V* characteristics because the states induced by current sweeping were very stable. The increase and decrease of conductance corresponding to the long-term potentiation and depression of synaptic weight, were respectively demonstrated by current sweepings and voltage pulses, as shown in Fig. 5.

5. Conclusion

Sputtered undoped and N doped Sb_2Te_3 films were investigated by x-ray diffraction and resistance measurements and the application to synaptic device was discussed. We can draw the following conclusions based on our experimental results.

(1) Mean crystal size decreased from 6.8 to 2.9 nm and thus crystal growth was significantly suppressed by fine nitrides due to N-doping.
(2) The resistivity of as-deposited N doped Sb_2Te_3 could be around 2-3 orders of magnitude higher than that of Sb_2Te_3.
(3) The N doped Sb_2Te_3 artificial intelligence synaptic device exhibited nonvolatility from the measured electrical characteristics.
(4) The long-term potentiation and depression of synaptic weight were demonstrated by current sweepings and voltage pulses, respectively.

Acknowledgements

This work was financially supported by Grant-in-Aid for Young Scientists from the Ministry of Education, Culture, Sports, Science and Technology of Japan (Nos. 24686042, and 21710135).

References

[1] W. A. Borders, H. Akima, S. Fukami, S. Moriya, S. Kurihara, Y. Horio, S. Sato and H. Ohno, Analogue spin–orbit torque device for artificial-neural-network-based associative memory operation, ***Appl. Phys. Exp.***, Vol. 10, 013007, 2017.

[2] A. El-Amin, K. Alexander, B. Rajendran, and R. Jhaa, Novel synaptic memory device for neuromorphic computing, ***Sci. Rep.***, Vol. 4, 5333, 2014.

[3] T. Ohno, T. Hasegawa, T. Tsuruoka, K. Terabe, J. K. Gimzewski, and M. Aono, Short-term plasticity and long-term potentiation mimicked in single inorganic synapses, ***Nature Materials***, Vol. 10, 591-595, 2011.

[4] S. G. Hu, Y. Liu, Z. Liu, T. P. Chen, Q. Yu, L. J. Deng, Y. Yin, and S. Hosaka, Synaptic long-term potentiation realized in Pavlov's dog model based on a NiOx-based memristor, ***J. Appl. Phys.***, Vol. 116, 214502, 2014.

[5] Y. Yin, and S. Hosaka, Controlled promotion of crystallization for application to multilevel phase-change memory, ***Appl. Phys. Lett.***, Vol. 100, 253503, 2012.

[6] B. Mun, B. You, S. Yang, H. Yoo, J. Kim, W. Park, Y. Yin, M. Byun, Y. Jung, and K. Lee, Flexible one diode-one phase change memory array enabled by block copolymer self-assembly, ***ACS Nano***, Vol. 9, 4120-4128, 2015.

[7] Y. Yin, Y. Zhang, Y. Takehana, R. Kobayashi, H. Zhang, and S. Hosaka, Sub 10 ns fast switching and resistance control in lateral GeTe-based phase-change memory, ***Jpn. J. Appl. Phys.***, Vol. 55, 06GG07, 2016.

[8] Y. Yin, and S. Hosaka, Controlled promotion of crystallization for application to multilevel phase-change memory, ***Appl. Phys. Lett.***, Vol. 100, 253503, 2012.

[9] S. Raoux, F. Xiong, M. Wuttig, and E. Pop, Phase change materials and phase change memory, ***MRS Bulletin***, Vol. 39, 703-710, 2014.